

## Influence of Axial Coolant Flow on Fuel Assembly Damping for the Response to Horizontal Seismic Loads

J. C. FLAMAND, J. C. MAGUIN, A. MATTEI

*CEA-CEN St Paul-lez-Durance, France*

J. RIGAUDEAU, J. C. LEROUX

*Fragema Lyon, France*

### 1. INTRODUCTION

The behaviour of a PWR reactor core under the effect of a horizontal earthquake is evaluated by Fuel Assembly (F/A) row models /1/. The results obtained, mainly the maximum compression force undergone by the spacer grids, are greatly dependent on the damping input into the F/A model.

The standard damping values are deduced from full-scale F/A tests, out of core, in air or in still water. The most significant values are obviously the in-water values, higher than in air, but no allowance is made for reactor coolant axial flow, which is also likely to increase damping. This phenomenon is primarily recognized for isolated tubes /2/, where the damping values are much lower than for F/A's (about 1 % of critical value as against 10 %). The aim of the study presented hereunder is to evaluate the relative importance of axial flow-induced damping on a F/A mock-up placed in a special-purpose flow channel ; the tests are performed in air, then in water at flowrates increasing up to a value comparable with that of the primary coolant at full reactor power.

### 2. MEASUREMENT PRINCIPLE

The mechanical properties of the tested assembly (natural frequency - damping) are deduced from its behaviour during a "snap-back" test : after a horizontal tension at a middle grid location, the F/A is released and damping is determined from the free lateral oscillations. Such a method yields a reduced value which is relative to the first mode, predominant in this response as well as in that to seismic loads.

These tests are conducted in several confinements, in air, in still water, in flowing water and for several initial displacement amplitudes.

### 3. DESCRIPTION OF TEST FACILITY

#### 3.1. Loop

The loop features :

- an underwater pump maximum capacity 270 m<sup>3</sup>/h for operation under a pressure head of 42 meters,
- a control valve and a by pass valve,
- an electromagnetic flowmeter,
- a water supply pit of about 20 m<sup>3</sup>.

The pit temperature is regulated by continuous water drainage and refilling.

#### 3.2. Test section

The test section is made of stainless steel. The 30 mm thick plexiglass front face, mounted inside a frame, is removable.

The confinements, varying with the required test configurations, take the form of P.V.C. plates which can be screwed into the test section. Note that this confinement variation is limited to that in F/A movement direction (section 4).

#### 3.3. Assembly

The mock-up consists of a 8 X 8 assembly 1.9 m in height, equipped with 5 Zircaloy grids. The assembly contains 60 rods and 4 guide thimbles ; despite its reduced size, the mock-up retains the overall structure of a PWR Fuel Assembly, particularly regarding the pitch, diameter and mechanical properties of the rods (Zircaloy cladding filled with pellets of a density equivalent to that of UO<sub>2</sub>).

#### 3.4. Assembly tension - release mechanism

The clamp transmitting the tensile force to the assembly is mounted around the 3rd spacer grid, at an elevation of 881 mm. It is welded around the grid such that there is no gap between it and the grid.

The trigger is connected to a tension system consisting of a screw providing a trigger forward and backward movement of about 13 mm.

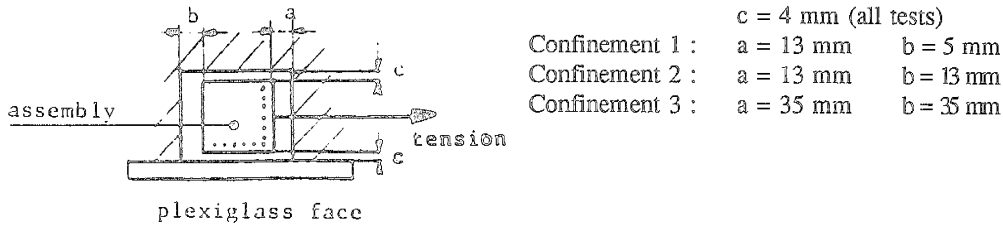
A lever integral with the trigger tilts the latter, allowing hook-up and release of the assembly.

#### 3.5. Measurement devices

Assembly displacement is measured through the plexiglass front face by means of a monitoring camera. For these tests, the measurement range is 24 mm with an accuracy of 2.4 μm.

4. TEST PARAMETERS : CONFINEMENT, AMPLITUDES AND WATER FLOWRATE

The various assembly test confinements are as follows :



For each of these confinements, tests were performed at variable amplitude (initial displacement) up to 12 mm :

- in air,
- in water at zero flow,
- in water for several fixed flowrates, corresponding to axial velocities up to 4.55 m/s.

5. DAMPING CALCULATION METHOD

The reduced damping value  $\beta$  is calculated by the logarithmic decrement method, i.e. from the equation :

$$\frac{\beta}{\sqrt{1 - \beta^2}} = \frac{1}{2 \pi k} \text{Ln} \left( \frac{A_1}{A_{1+k}} \right)$$

where  $A_1$  and  $A_{1+k}$  are the values either of two maximum values or two minimum values in the displacement free oscillations, with a time interval of  $k$  pseudo-periods.

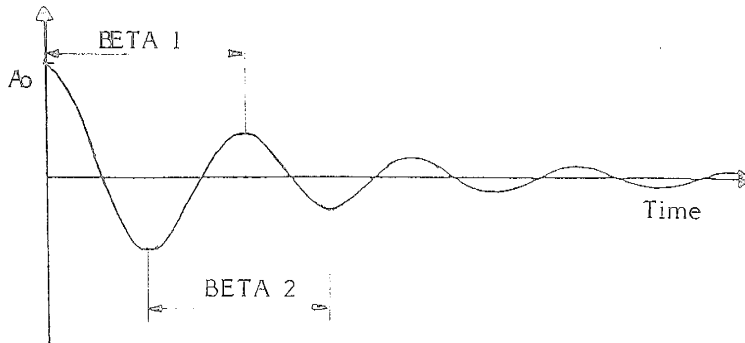
Since relatively large damping values are obtained in this study, the usual explicit formula where  $\beta^2$  is neglected may lead to errors which are not completely negligible ; for the same reason, the two first periods only can be used for damping determination.

Two different determinations have been performed, both on a single period :

- $\beta_1$ , between the initial displacement considered as positive, and the first maximum value (first period),
- $\beta_2$ , between the first and second minimum values (first "free" period),

as displayed on the following figure.

Amplitude of displacement



As damping is amplitude dependent,  $\beta_1$  represents the damping value corresponding the closest to the initial displacement, which is taken as the reference amplitude ( $x$ - value in damping vs. amplitude diagrams), but it is dependent on uncertainties related to the drop conditions.  $\beta_2$ , which is often used in core seismic analysis, is free from such uncertainties, yet this damping value is not associated with the reference initial amplitude, more particularly when damping becomes large. Therefore results provided by both determinations are presented.

## 6. TEST RESULTS

### 6.1. First natural frequency

Figure 1 displays typical features of F/A frequencies, also observed in full-scale tests : a frequency decrease when amplitude increases, because of rod slippage in grid cells (non-linear behaviour), and a decrease for in-water tests with respect to in-air tests, due to the added mass effect. Influence of axial flow and of confinement is negligible.

### 6.2. Damping variation with test conditions (determination of $\beta_1$ )

All  $\beta_1$  values are presented on figure 2. As with frequency decrease, the damping increase with increasing amplitude results from rod slippage in grid cells and it reaches a maximum value for large amplitudes. The variation is quite similar to that obtained for full-scale F/A tests.

Damping is found to be larger in still water than in air, yet this increase is much smaller than the dramatic one observed under axial flow : for a 10 mm amplitude,  $\beta_1$  in air is about 18 % of critical damping value, 25 % in still water, i.e. + 30 % relative increase, and 45 % of critical damping value at maximum velocity, i.e. + 80 % relative increase with respect to still water conditions. The effect of axial flow is therefore largely predominant.

The influence of confinement in the movement direction is found to be small.

### 6.3. Comparison between $\beta_1$ and $\beta_2$ determinations

Figure 3 displays similar variations of  $\beta_1$  and  $\beta_2$  with amplitude and axial flow, which confirms the results presented in section 6.2. Yet  $\beta_2$  is always smaller than  $\beta_1$ , because of the smaller amplitudes during the period used for determination. Then the difference between  $\beta_1$  and  $\beta_2$  logically increases with damping, and the strong influence of axial flow would be actually minimized by considering  $\beta_2$  only.

## 7. CONCLUSIONS

The existence of a large damping increase under axial flow is clearly demonstrated by test results. Therefore this phenomenon concerns not only isolated tubes, but also rod bundles with multiple support such as fuel assemblies, and it may represent a large conservatism margin when not allowed for in their modelling.

Test results also demonstrate that the mock-up behaviour is representative of that of a full-scale assembly, and that actual confinement conditions are not of much concern since their influence remains small. However, applying test results under axial flow to a core model can be envisaged only with caution, since no clear physical interpretation of this phenomenon has been found (at least for such large damping values). Further studies will comprise a complementary experimental program, in order to specify the physical nature and the application range of this effect, and to provide hints for a theoretical interpretation.

## REFERENCES

- /1/ CALLENS, C., LEROUX, J.C., RIGAUDEAU, J., 1991 - Status of Methods for Justifying Fuel Assembly Lateral Strength during an Earthquake, Paper C 6/1, SMIRT-11.
- /2/ WAMBSGANSS, M.W., CHEN, S.S., 1972 - Tentative Design Guide for Calculating the Vibration Response of Flexible Cylindrical Elements in Axial Flow - ASME Pressure Vessel and Piping : Design and Analysis, a Decade of Progress, Vol. 2.

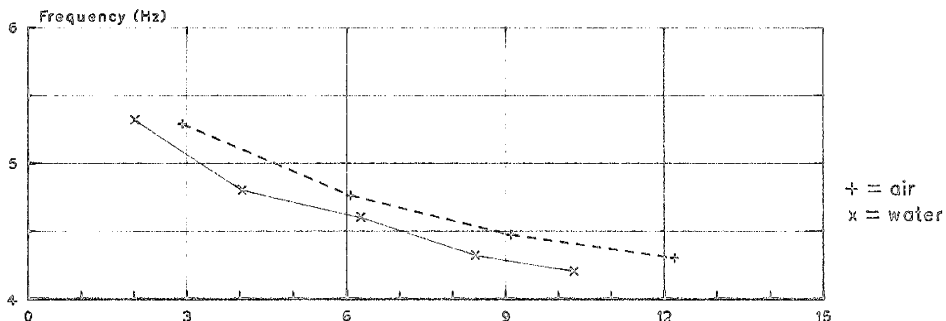


Fig. 1 First natural frequency versus initial amplitude of displacement

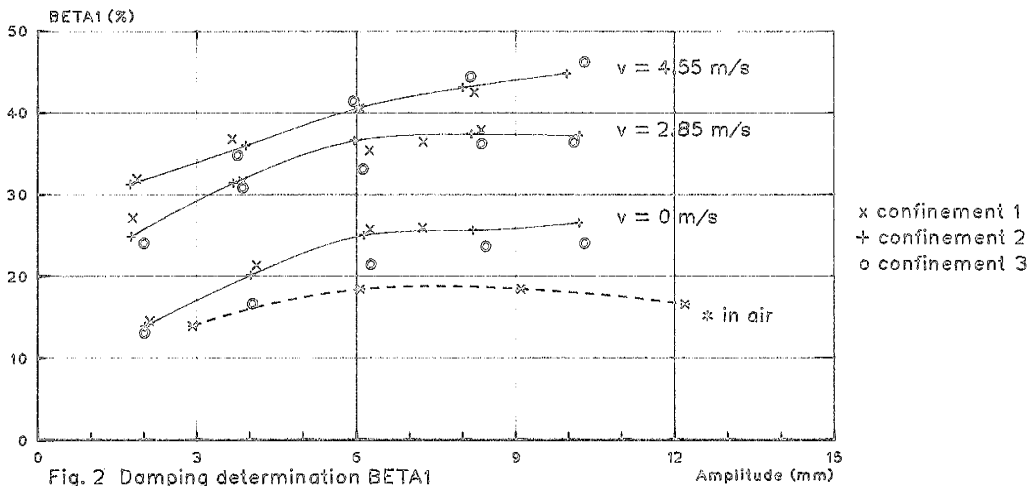


Fig. 2 Damping determination BETA1 versus initial amplitude of displacement

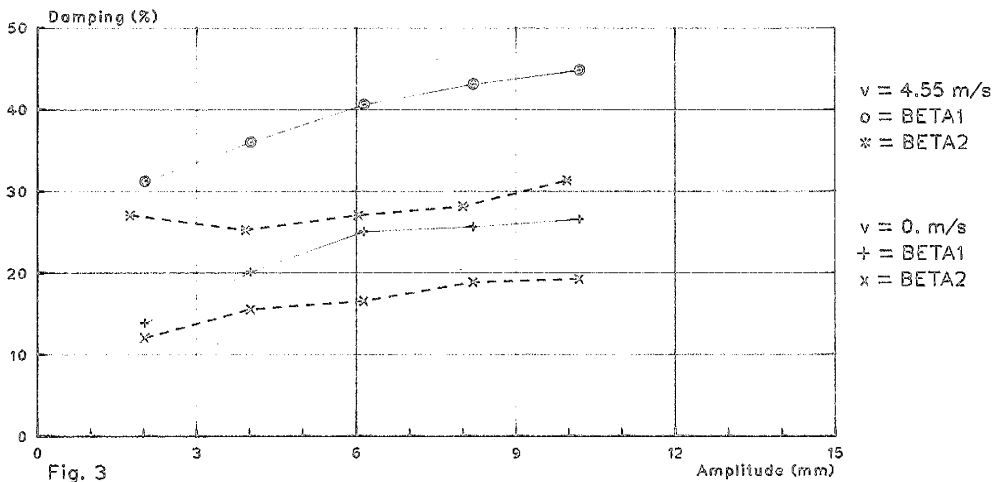


Fig. 3 Comparison between BETA1 and BETA2 for confinement 2